Extended Hamiltonian theory of the fractional quantum Hall effect: Collective edge modes at fractional filling

Hoang K. Nguyen[1], Yogesh N. Joglekar[2], and Ganpathy Murthy[1]
[1]*Department of Physics and Astronomy, University of Kentucky, Lexington, KY 40506,*
[2] *Theoretical Division, Los Alamos National Laboratory, Los Alamos, NM 87544.*
(Dated: March 2, 2004)

Over the past few years one of us in collaboration with R. Shankar has developed an extended Hamiltonian formalism capable of describing the ground state and low energy excitations in the fractional quantum Hall regime. The Hamiltonian, expressed in terms of Composite Fermion operators, incorporates all the nonperturbative features of the fractional Hall regime, so that conventional many-body approximations such as Hartree-Fock and time-dependent Hartree-Fock are applicable. In this paper we apply this formalism to study the collective edge modes of systems at the principal fractions $\frac{1}{3}$, $\frac{2}{5}$, and $\frac{1}{5}$ for systems with unreconstructed edges. The primary advantage of the method is that one works in the thermodynamic limit right from the beginning, thus avoiding the finite-size effects which ultimately limit exact diagonalization studies.

PACS numbers:

I. INTRODUCTION

The bulk fractional quantum Hall effect is by now well-understood as resulting from an interaction-driven incompressible state[1–3] of the two-dimensional electron gas (2DEG). It was also realized long ago[4] that the edges of the bulk system play a fundamental role in transport at low frequencies. Since the bulk is incompressible and gapped, only the gapless edge modes are excited at low frequencies. An effective description of edge excitations for incompressible fractions was first proposed by Wen[5]. He developed a hydrodynamic theory of a sharp edge, which is a realization of the one-dimensional Chiral Luttinger Liquid (CLL) model.

Recently, several high-precision experiments[6,7] have probed the low-frequency dynamics of the edge in the fractional quantum Hall (FQH) regime over a range of filling factors. Some features of the results, such as the observation of a power law in the $I - V$ curve which depends on the filling factor, and the actual magnitude of the power-law exponent[6], are unexpected from the point of view of hydrodynamic theories of the edge[5,8]. Many explanations have been proposed for these discrepancies[9–16], including the effects of long-range interactions and edge reconstructions.

Motivated by these experiments, there have been recent numerical exact diagonalization studies[14] to explore the effects of edge reconstructions on the behavior of the collective modes. While important qualitatively new results[16] have been obtained by this research, these studies do suffer from finite-size effects.

We want to investigate the physics of FQH edges using the extended Hamiltonian theory (EHT) developed by Shankar and one of us[17]. This approach has the advantage that it starts with a microscopic Hamiltonian, permits analytic calculations in the thermodynamic limit and it also retains the lowest Landau level (LLL) limit. It thus provides a complementary approach to that of exact diagonalizations. In a previous report[18], we applied the EHT to study the structure of FQH edges within the Hartree-Fock (HF) approximation. In this paper, we further explore the edges beyond mean-field level. The method to be used is the time-dependent Hartree-Fock (TDHF) approximation which systematically incorporates particle-hole states. It also turns out to be a conserving approximation[19], in that it respects the symmetries of the problem.

The structure of our paper is as follows: In the next section, we review the essentials of the EHT and the mean-field calculations of FQH edges. The time-dependent Hartree-Fock approximation is described in the Section 3. Our numerical results for $\nu = \frac{1}{3}$, $\frac{1}{5}$ and $\frac{2}{5}$ are presented in Section 4. The results for $\frac{2}{5}$ are, to the best of our knowledge, the first in the literature. The last section contains conclusions and caveats. Throughout this paper we restrict ourselves to unreconstructed edges due to computational limitations of our own.

II. EXTENDED HAMILTONIAN THEORY AND HARTREE-FOCK APPROXIMATION

In a strong magnetic field, the kinetic energy of electrons is quenched. Single-particle states are organized into Landau levels separted by the cyclotron energy, $\hbar\omega_c$. The interacting Hamiltonian of the system is simply:

$$H_e = \frac{1}{2}\int d^2q \; v(\vec{q})\rho_e(\vec{q})\rho_e(-\vec{q}) \tag{1}$$

where $v(\vec{q})$ is the electron-electron interaction. The interaction energy scale is typically several tens of Kelvins, of the same order as the cyclotron energy (about $100K$). Nevertheless, it is usually treated as a perturbation on the ground state Slater determinant of ν Landau levels comptely filled. For a fractional filling, however, this ground state is degenerate and the perturbative approach fails[1]. The key insight of Jain[2] was that if one thinks in terms of Composite Fermions (CFs), which are envisioned as electrons attached to an even number $2s$ of flux quanta, one can recover an independent particle picture. In this approach in a system at filling factor $\nu = p/(2ps+1)$, the CFs see an effective field $B^* = B/(2ps+1)$, which is just right for them to fill p CF-Landau levels (CF-LLs). Based on this insight, Jain constructed excellent wavefunctions for ground and low-lying excited states for the principal fractions.

It was soon realized that in order to calculate response functions or finite-temperature properties, one needs a dynamical theory. Initial attempts focused on bosonic[20] or fermionic[21] variants of the Chern-Simons (CS) theory[22], culminating in a CS theory for $\nu = \frac{1}{2}$[23], which is a Fermi-liquid-like state[24]. However, these theories, while satisfactory in many respects, still did not incorporate some of the nonperturbative aspects of the CF, such as the fact that in the lowest Landau level limit its effective mass should be determined by the interactions alone, or that its charge should be fractional.

To handle these problems, Murthy and Shankar developed the extended Hamiltonian theory[17], a detailed account of which can be found in a recent review[25]. A key ingredient of this theory is the introduction of a new set of coordinates of *pseudo-vortices*, in addition to those of electrons. For a FHQ liquid at filling fraction $\nu = p/(2ps+1)$ where p and s are integer, each electron couples with $2s$ pseudo-vortices to form a composite fermion (CF) in the following way:

$$\vec{R}_e = \vec{r} - \frac{l^2}{1+c}\hat{z}\times\vec{\Pi}, \tag{2}$$

$$\vec{R}_v = \vec{r} + \frac{l^2}{c(1+c)}\hat{z}\times\vec{\Pi}, \tag{3}$$

where $c^2 = 2\nu s$, and $\vec{r}$ and $\vec{\Pi}$ are the position and velocity operators of the composite fermion. The electron guiding center $\vec{R}_e$ and the pseudo-vortex guiding center $\vec{R}_v$ satisfy the algebra

$$\begin{aligned} [R_{e\alpha}, R_{v\beta}] &= 0, \\ [R_{e\alpha}, R_{e\beta}] &= -il^2\epsilon_{\alpha\beta}, \\ [R_{v\alpha}, R_{v\beta}] &= +i\frac{l^2}{c^2}\epsilon_{\alpha\beta}. \end{aligned} \tag{4}$$

The electron guiding-center coordinates satisfy the magnetic algebra with charge $-e$, whereas the pseudo-vortex guiding-center algebra represents an object with charge $+ec^2$. The CFs thus have a magnetic algebra charge of $e^* = -e(1-c^2)$, showing that they are subject to a reduced magnetic field $B^* = B/(2ps+1)$, just right to fill the first p CF-Landau levels, exactly as in Jain's picture[2]. The Hartree-Fock state of CFs with the first p LLs filled provides a *non-degenerate* starting point for analytical calculations.

To calculate the matrix elements of these operators in the CF basis, we use the single-particle states of the composite fermions in the reduced effective field B^*. In the Landau gauge, a single-particle state $|nX\rangle$ is characterized by the CF-Landau level index n and the guiding-center coordinate X. In the real-space representation, the (un-normalized) single-particle wavefunction is

$$\langle\vec{r}|nX\rangle = e^{iXy/l^{*2}}e^{-(x-X)^2/2l^{*2}}H_n\left[(x-X)/l^*\right], \tag{5}$$

where $H_n(x)$ are the Hermite polynomials and $l^* = \sqrt{h/eB^*}$ is the magnetic length in the reduced field B^* seen by the CFs. Using this basis, it is straightforward to express the electron density ρ_e and the pseudo-vortex density ρ_v operators in second-quantized notation:

$$\rho_e(\vec{q}) = \sum_{\nu X} e^{-iq_xX} d^\dagger_{n_1X-Q_yl^*/2} d_{n_2X+Q_yl^*/2}\rho_{n_1n_2}(\vec{q}) \tag{6}$$

$$\rho_v(\vec{q}) = \sum_{\nu X} e^{-iq_xX} d^\dagger_{n_1X-Q_yl^*/2} d_{n_2X+Q_yl^*/2}\chi_{n_1n_2}(\vec{q}) \tag{7}$$

where $d_{nX}, d^\dagger_{nX}$ are canonical fermion operators which destroy and create CF's in the state $\{n, X\}$, and the matrix elements are

$$\rho_{n_1 n_2}(\vec{q}) = (-1)^{n_< + n_2} \sqrt{\frac{n_<!}{n_>!}}\, e^{i(n_1-n_2)(\theta_q - \pi/2)} \times (cQ/\sqrt{2})^{|n_1-n_2|}\, e^{\frac{-Q^2}{4}} L_{n_<}^{|n_1-n_2|}(c^2Q^2/2), \tag{8}$$

$$\chi_{n_1 n_2}(\vec{q}) = (-1)^{n_< + n_2} \sqrt{\frac{n_<!}{n_>!}}\, e^{i(n_1-n_2)(\theta_q - \pi/2)} \times (Q/c\sqrt{2})^{|n_1-n_2|}\, e^{\frac{-Q^2(2-c^2)}{4c^2}} L_{n_<}^{|n_1-n_2|}(Q^2/2c^2). \tag{9}$$

Here $c = \sqrt{2\nu s}, Q = ql^*, n_<(n_>)$ is the lesser (greater) of n_1, n_2, and L_n^k are the Laguerre polynomials. We shall set l^* as the unit of length in the rest of the paper, i.e., dropping the notation of l^* in the formulae.

We have now expressed the electron density operators, and hence the microscopic Hamiltonian for the fractional quantum Hall systems, in terms of CF operators, d_{nX} and $d^\dagger_{nX}$. Therefore the original problem of interacting electrons in the *fractional* quantum Hall regime has been readily transformed into a problem of CFs in the *integer* quantum Hall regime where various many-body approximations are applicable. We must, however, note that there is no free lunch. The price to pay is that the transformed problem is subject to special constraints as a result of the introduction of the pseudo-vortex coordinates. Dealing with the constraints is the content of Section III in our paper.

We next consider a background charge $\rho_b(x)$ to produce a confining potential along with $x = 0$. The Hamiltonian is modified by the following term:

$$H_b = \sum_{\vec{q}} V_{eb}(-\vec{q})\rho_e(\vec{q}) \tag{10}$$

with

$$V_{eb}(x) = \int_{-\infty}^{\infty} dx'\, v_{eb}(x-x')\rho_b(x'), \tag{11}$$

and $v_{eb}(x)$ is the electron-background interaction. The background charge-density is chosen to vanish linearly over width W, as in the analysis of Chamon and Wen[26] on the $\nu = 1$ edge: $\rho_b(x) = 0$ for $x < -W/2$, $\rho_b(x) = -\frac{\rho_0}{2}\left[1 + \frac{2x}{W}\right]$ for $|x| < W/2$, and $\rho_b(x) = \rho_0$ for $x > W/2$ where ρ_0 is the CF density in the bulk. We also set the electron-background interaction, v_{eb}, to be identical to that between electrons, v.

In the bulk of a FQH liquid of filling $\nu = p/(2ps+1)$, p CF-Landau levels are competely filled. Due to the presence of the confining potential, close to the edge, different CF-Landau levels mix together. Since there is still translation invariance in the y-direction, the Landau gauge quantum number X is still a good quantum number, and only CF-LLs with the same X will mix. Mixing matrices $\alpha(X)$ as function of X are introduced:

$$d_{nX} = \sum_m \alpha_{nm}(X) a_{mX} \tag{12}$$

The total Hamiltonian, $H_e + H_b$, represented in terms of new operators a_{mX} and $a^\dagger_{mX}$, is decoupled by the standard procedure

$$a^\dagger_\alpha a^\dagger_\beta a_\gamma a_\delta \to \langle a^\dagger_\alpha a_\delta\rangle a^\dagger_\beta a_\gamma + \langle a^\dagger_\beta a_\gamma\rangle a^\dagger_\alpha a_\delta - \langle a^\dagger_\alpha a_\gamma\rangle a^\dagger_\beta a_\delta - \langle a^\dagger_\beta a_\delta\rangle a^\dagger_\alpha a_\gamma. \tag{13}$$

while the mean-field condensate is chosen to be

$$\langle a^\dagger_{mX} a_{nX'}\rangle = \delta_{mn}\delta_{XX'} N_m^F(X) \tag{14}$$

where $N_m^F(X)$ is the CF-occupation number at orbital X and CF-Landau level m. Note that with this decoupling scheme, we are explicitly forbidding any structure in the y-direction. Upon decoupling, the mean-field Hamiltonian becomes

$$H^{HF} = \sum_{mnX} H_{mn}(X) a^\dagger_{mX} a_{nX} \tag{15}$$

The mixing matrices α's are determined to make H^{HF} diagonal. The process is normally carried out iteratively as in our previous work.[18] The quantities of interest in mean-field study are the energy band $E_m(X) = H_{mm}(X)$, the occupation function $N^F_m(X)$, and the mixing matrix $\alpha_{m1m2}(X)$.

III. TIME-DEPENDENT HARTREE-FOCK (CONSERVING) APPROXIMATION

A. Time-dependent Hartree-Fock Hamiltonian

As mentioned in the previous section, special care is required in treating the transformed Hamiltonian. In particular, the original electronic Hamiltonian knows nothing about the vortex density, ρ_v, and thus is indifferent with respect to our choice of ρ_v. The transformed problem has extra degrees of freedom, the pseudovortex coordinates. Exact solutions to this problem will automatically be degenerate along the pseudovortex manifold, and will thus have a gauge symmetry. However, the mean-field ground state does not have the required gauge invariance. The situation is similar in the theory of superconductivity, where the BCS ground state is not gauge invariant. Nonetheless, a gauge-invariant approximation to the dynamical response can still be obtained from the mean-field ground state by a so-called conserving approximation[19]. TDHF turns out to be the simplest one of the class of conserving approximations, and is standard in the superconductivity context to deal with the gauge symmetry[19]. Read[27] was the first to apply the TDHF method to study the problem of $\nu = 1$ bosons, which has important similarities to electronic half-filled FQH system[24]. Murthy subsequently used the TDHF approximation to find the collective modes for the incompressible fractions using the EHT.[28]

In this Section, we will exploit the TDHF approximation to derive the dispersion relations of the edge excitations. The way the conserving nature of the TDHF approximation manifests itself is that the spectrum of the TDHF Hamiltonian neccessarily contains zero eigenvalues, each corresponding to an unphysical gauge degree of freedom, while the rest of the spectrum is physical.[28] It is important that the unphysical zero-modes are identified and excluded, which is the task of the next section.

Due to (4), $[\rho_e(\vec{q}), \rho_v(\vec{q}')] = 0$. The total Hamiltonian, $H_e + H_b$, therefore commutes with ρ_v. Consider the magnetoexciton operator

$$O_{m_1 m_2}(X, Q_y) = a^\dagger_{m_1, X-Q_y/2} a_{m_2, X+Q_y/2} \tag{16}$$

where a is the *rotated* annihilation operator related to the CF-operator d as in Eq. (12). We have explicitly made use of the fact that there si translation invariance in the y-direction, and therefore $Q_y = q_y (l^*)^2$. Since Q_y is a good quantum number, we shall suppress the index Q_y and simply write $O_{m_1 m_2}(X)$. The equation of motion for the magnetoexciton operator is

$$-i \frac{\partial}{\partial t} O_{m_1 m_2}(X) = [H, O_{m_1 m_2}(X)] \tag{17}$$

Applying the standard HF decoupling procedure, Eq. (13), to the right-hand-side:

$$\begin{aligned}
[H, O_{m_1 m_2}(X_0)] \;\to\; & [E_{m_1}(X_0 - Q_y/2) - E_{m_2}(X_0 + Q_y/2)] O_{m_1 m_2}(X_0) + [N^F_{m_1, X_0 - Q_y/2} - N^F_{m_2, X_0 + Q_y/2}] \times \\
& \times \sum_{X,\nu,\kappa,\kappa'} \left[h_{k_1 k_2' k_1' k_2}(-Q_y, X_0 - X) - h_{k_1 k_2 k_1' k_2'}(X - X_0, Q_y) \right] \times \\
& \times \; \alpha^\star_{k_1 n_1}(X - Q_y/2) \alpha_{k_2 n_2}(X + Q_y/2) \alpha^\star_{k_1' m_2}(X_0 + Q_y/2) \alpha_{k_2' m_1}(X_0 - Q_y/2) O_{n_1 n_2}(X)
\end{aligned} \tag{18}$$

where

$$h_{k_1 k_2 k_1' k_2'}(X, Q_y) = \int \frac{dq_x}{2\pi} v(\vec{q}) \rho_{k_1 k_2}(\vec{q}) \rho_{k_1' k_2'}(-\vec{q}) e^{-i q_x X} \tag{19}$$

and $\mu = (m_1, m_2)$, $\nu = (n_1, n_2)$ and so on, for short. Define a vector $\Psi_\mu(X)$ corresponding to the operator

$$O_\Psi = \sum_{\mu X} \Psi_\mu(X) O_\mu(X). \tag{20}$$

In the space spanned by O_Ψ, the TDHF Hamiltonian reads

$$\begin{aligned}\mathcal{H}(\mu,\nu;X_0,X;Q_y) \;=\; & \delta_{m_1n_1}\delta_{m_2n_2}[E_{m_1}(X_0-Q_y/2)-E_{m_2}(X_0+Q_y/2)]+[N^F_{m_1,X_0-Q_y/2}-N^F_{m_2,X_0+Q_y/2}]\times \\ & \times\sum_{\kappa,\kappa'}\left[h_{k_1k_2'k_1'k_2}(-Q_y,X_0-X)-h_{k_1k_2k_1'k_2'}(X-X_0,Q_y)\right]\times \\ & \times\;\alpha^\star_{k_1n_1}(X-Q_y/2)\alpha_{k_2n_2}(X+Q_y/2)\alpha^\star_{k_1'm_2}(X_0+Q_y/2)\alpha_{k_2'm_1}(X_0-Q_y/2) \end{aligned} \tag{21}$$

The TDHF Hamiltonian is the key quantity containing information about the collective modes in the system. Upon diagonalization, we obtain the energy spectrum of excitations, and the left- and right-eigenvectors. Direct inspection of (19, 21) shows that $\mathcal{H}$ changes sign as Q_y does (after a suitable reshuffling of the indices). That means the spectrum at a Q_y contains information about $-Q_y$ as well. Left- (right-) eigenvectors are identical for both $\pm Q_y$. We are interested in the gapless excitations across the edge. These modes are in the regime of low energy and momentum. The task at hand is to identify these modes from the energy spectrum and will be addressed in the next subsection.

B. Identification of physical modes

Due to the gauge symmetry of the original Hamiltonian, it can be shown that the TDHF Hamiltonian $\mathcal{H}$ neccesarily has zero eigenvalues, even for a nonuniform system. In the full account, each energy level of H is infinitely degenerate since it costs no energy to rotate among gauge-connected eigenstates. The zero modes of $\mathcal{H}$ are thus unphysical (or spurious) and need to be discarded from its spectrum. We stress that the spurious modes only have precisely zero energy when a full set of infinite CF-LLs are taken into account. Obviously, in computations, though one tries to include as many CF-LLs as possible, that number cannot be infinite. A technical problem of how to separate the unphysical modes from the physical ones arises.

There are two different ways to achieve this. Firstly, one can monitor the behavior of the energy of a mode. As more CF-LLs are added, the energy of an unphysical mode gets closer to zero while that of a physical mode becomes stable. In the bulk case, Murthy successfully singled out the unphysical modes[28] using this procedure. Secondly, one can resort to the electron density correlation function: Since the electron density operator is gauge-invariant, unphysical modes should decouple from its correlation functions as more CF-LLs are added.

In the edge case, the first method is impractical. This is because the energy spectrum of $\mathcal{H}$ contains every mode at a given Q_y, including many unphysical modes which are at high x-momenta and require a very large number of CF-LLs to be detected. We shall use the second method in the edge problem as explained in what follows.

The electron density-density correlation is

$$S(X_0,X_0',Q_y,\omega)=-i\langle\rho_e(X_0,Q_y,\omega)\rho_e(X_0',-Q_y,-\omega)\rangle, \tag{22}$$

ground-state expectation of a four-fermion operator. Detailed calculations give rise to a formula for the density coorelator in terms of known quantities:

$$\begin{aligned}S(X_0,X_0',q_y,\omega) \;=\; & \frac{L^2}{2\pi}\sum_\alpha\sum_\kappa\left(\sum_{\mu X}\rho_{m_1m_2}(X_0-X,q_y)\psi^{R(\alpha)}_{k_1k_2}(X,Q_y)\alpha^\dagger_{m_1k_1}(X-Q_y/2)\alpha_{m_2k_2}(X+Q_y/2)\right)\times \\ & \times\left(\sum_{\nu X'}\rho_{n_1n_2}(X_0'-X',-q_y)\psi^{L(\alpha)}_{k_4k_3}(X',-Q_y)\alpha^\dagger_{n_1k_3}(X'+Q_y/2)\alpha_{n_2k_4}(X'-Q_y/2)\right)\times \\ & \times\;\frac{1}{\omega-E_\alpha+i\eta\; sign(E_\alpha)}\left[N^F_{k_3}(X'+Q_y/2)-N^F_{k_4}(X'-Q_y/2)\right] \end{aligned} \tag{23}$$

where $\rho_\mu(X,Q_y)$ is the $1D$ Fourier transform of the matrix element defined in Eq. (8):

$$\rho_\mu(X,q_y)=\int dq_x\, e^{iq_xX}\rho_\mu(q_x,q_y) \tag{24}$$

As handy as it looks, Eq. (23) still has a minor technical problem. It describes how strongly a mode couples with the electron density; in other words, while it does discriminate between physical and unphysical modes, it does not discriminate between the bulk and edge modes. We note that physical edge modes at low momentum and energy, the regime of interest, should become stable as more and more CF-LLs are added. In a further refinement, we exclude the high momentum-modes by a filtering procedure. Instead of a pure electron density, ρ_e, to be used in (22), consider a filtered operator concentrated near the edge

$$\rho_\mu^f(X_0, q_y) = \sum_X e^{-(X-X_0)^2/2l_f^2}\ \rho_\mu(X, q_y) \tag{25}$$

that cuts off all fluctuations (in $x-$direction) faster than $1/l_f$. The choice of Gaussian filtering in (25) is convenient for calculations. The results we present are all based on the choice $l_f = l^*$, which seems to work well. The filtered density correlator, $S^f(X_0, X_0', q_y, \omega) = -i\langle \rho_e^f(X_0, q_y, \omega)\rho_e^f(X_0', -q_y, -\omega)\rangle$ satisfies exactly the same formula (23) except the matrix elements $\rho_\mu(X, Q_y)$ are replaced by the filtered ones, $\rho_\mu^f(X, Q_y)$, defined as

$$\rho_\mu^f(X, q_y) = \int dq_x\ e^{iq_x X - q_x^2 l_f^2/2}\rho_\mu(q_x, q_y) \tag{26}$$

IV. RESULTS

In our following calculations, we set the edge to be parallel to the $y-$axis. The background charge density, and thus the confining potential, is a function of x. We vary the confining potential by changing the width W over which the background charge is linearly smoothen. For the interaction, we considered both short-range and long-range interactions. The short-range interaction was chosen to be Gaussian for analytical convenience

$$v(\vec{q}) = e^{-q^2\lambda^2/2}, \tag{27}$$

where $\lambda = l^\star$. In addtion, in $\nu = 1/3$ case, we considered the long-range Thomas-Fermi potential

$$v(\vec{q}) = \frac{2\pi}{\sqrt{Q^2 + Q_{TF}^2}}, \tag{28}$$

where $Q_{TF} = q_{TF}l^\star = 0.4$. The long-range case is considerably more difficult for the HF part of the calculation. As Q_{TF} decreases, it takes more iterations for HF to converge, and the presence of the edge makes itself felt deeper inside the bulk. As we will describe, we did not find any substantive differences in hte edge collective modes between the two cases. This being the case, we concentrated on the short-range case for $\frac{2}{5}$ and $\frac{1}{5}$.

Deep in the bulk, the quantum Hall liquid is uniform and the structure of CF-LLs and excitations in TDHF is understood.[28] For numerical purposes, we focus on the region around the edge, taking $8\,l^\star$ in the bulk side and $2\,l^\star$ in the empty side. The lattice spacing is $\Delta x = 0.1\,l^\star$, resulting 100 sites. Typically, 8 to 10 CF-LLs are considered. The TDHF Hamiltonian size is of order a few thousand, making the diagonalization feasible.

Notice that Δx sets the lower bound of resolution for Q_y (recall that the magnetoexciton contains CF creation and destruction operators of Q_y separation.) We believe that our choice of $\Delta = 0.1\,l^\star$ is appropriate as the natural length scale in the problem is $l^\star$. Reducing Δx, while allowing us to explore smaller Q_y, would require more computational resources.

The filling fraction $\nu = 1/3$ corresponds to $s = 1, p = 1$, or $c = \sqrt{2/3}$ in equations (3,3). The ground state in the bulk has only the lowest CF-LL filled. We first repeated the mean-field calculation to obtain the energy bands, the mixing matrix, and the occupation profile. From these quantities, the TDHF Halmitonian, $\mathcal{H}$, is created as in Eq. (21) and diagonalized. Direct inspection of $\mathcal{H}$ reveals that only the excitations from the lowest CF-LL to higher ones are relevant to the edge modes. We thus need to keep only elements in $\mathcal{H}$ that has m_1 or m_2 vanishing. The size of the TDHF Hamiltonian at 10 CF-LLs is $100 \times 19 = 1,900$ rows (and $1,900$ columns.) While diagonalizing such a matrix is easy, the most time-consuming part is the setup of $\mathcal{H}$ due to the quadruple sum in Eq. (21).

The TDHF Hamiltonian is not symmetric. Remarkably, our diagonalization results find that it only possesses *real* eigenvalues, meaning that every mode is *long-lived* as normally expected. Upon diagonalization, the set of left- and right- eigenvectors are used to compute the filtered density correlator. We present in Fig. 2 the imaginary part of $S^f(0, 0, Q_y = 0.3, \omega)$ at $W = 0$ for Gaussian interaction at 8 and 10 CF-LLs. As is evident in the picture, while there are several peaks at 8 CF-LLs, many of them at low energy disappear at 10 CF-LLs. These peaks are spurious modes which decouple from the electron density in the limit of infinite number of CF-LLs. The arrows indicate the peaks of physical modes which are *stable* as more CF-LLs are added. The peak of positive energy is the edge mode, it has little change in position and weight. The gradual disappearance of unphysical modes and the stability of the physical modes with respect to CF-LL number are strong indications that our calculations are reliable.

By carrying out this procedure for different values of Q_y, one can find the dispersion relation for the $\nu = 1/3$ edge mode at $W = 0$, Gaussian interaction, 10 CF-LLs, which is shown in Fig. 4. The dotted line is the (naive)

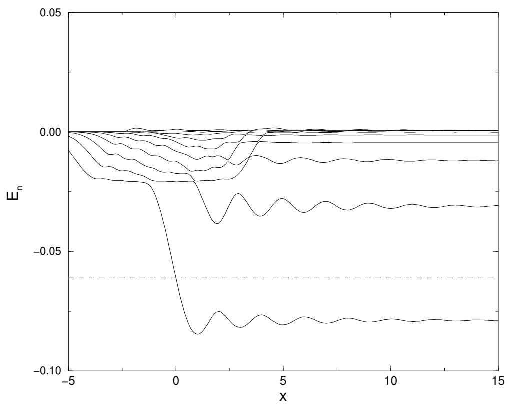

FIG. 1: Mean-field energy bands for 10 (solid) CF-LLs at $\nu = 1/3$, $W = 0$, Gaussian interaction. The energy is in units of $e^2/\varepsilon l^*$, and the x-axis is in units of l^*. Note that our interaction potential is un-normalized. The dotted line denotes the chemical potential. In the bulk only one CF-LL is occupied.

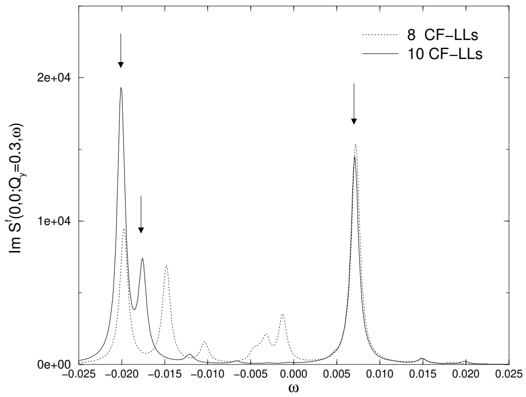

FIG. 2: Electron density-density correlator for 8 (dotted) and 10 (solid) CF-LLs at $\nu = 1/3$, $Q_y = 0.3$, $W = 0$, Gaussian interaction. Once again the frequency is in units of $e^2/\varepsilon l^*$. The arrows indicate poles of the physical edge modes. Notice that unphysical modes lying between the peaks strongly decouple from electron density at 10 CF-LLs, whereas the physical (edge) mode with positive energy remains unchanged in both position and weight.

mean-field excitation of the edge. The TDHF approximation, by taking into account particle-hole pair states, reduces the mean-field energy as can be seen in the figure. The edge mode is gapless, as expected. At very small momentum, its should be linear, $\omega = v\,q$, where v is the cyclotron velocity of CF along the edge. For larger momentum, we presume a momentum-dependent velocity, $v(q)$. To see heuristically what the natural form of this velocity might be, note that as Q_y increases, we are making excitations deeper into the empty region. In this region, the electron density is smaller than in the bulk, and thus the effective field seen by the CFs must be larger. This means the velocity of excitations must be smaller. Assuming a linear variation of the electron density (and thus the effective field) near the edge, as seen in Fig. (3), we arrive at the following form:

$$\omega = \frac{v_0\, q\, l^*}{1 + a\, v_0\, q\, l^*}, \tag{29}$$

where v_0 is the cyclotron velocity at $q = 0$, and a is constant.

We rewrite (again, in units where $l^* = 1$):

$$\frac{q}{\omega} = \frac{1}{v_0} + a\, q. \tag{30}$$

Fig. 5 shows the ratio q/ω, the CF cyclotron velocity inverse, as function of momentum. The data seem to fit our heuristic form.

Now we examine how the collective mode dispersion is affected when the width of the confining potential W is increased. Data for $W = 1.2\, l^\star$ ($\nu = 1/3$) are shown in Figs. 6 and 7. Notice the appreciable softening in the

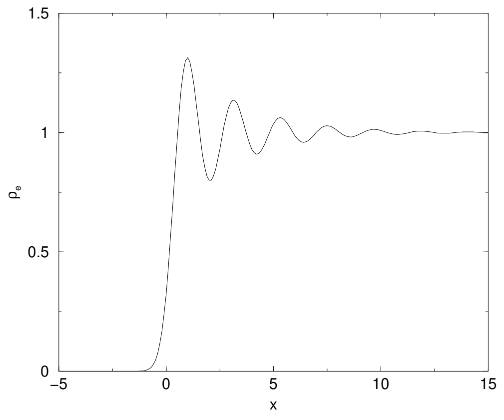

FIG. 3: Electron density profile at $\nu = 1/3$, $W = 0$, Gaussian interaction, 10 CF-LLs involved. The x-axis is in units of l^*. The asymptotic value of 1 in the bulk signifies that 1 CF-LL is filled in the bulk.

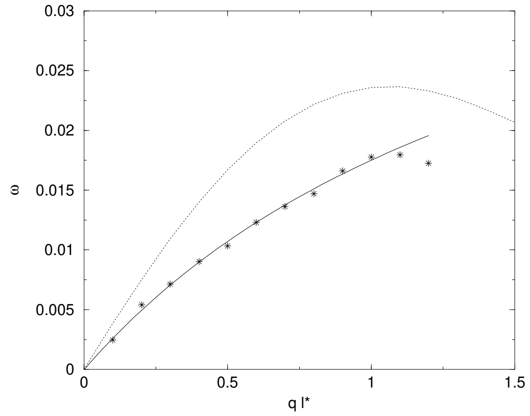

FIG. 4: Dispersion of $\nu = 1/3$ edge mode at width $W = 0$, Gaussian interaction, 10 CF-LLs. The dotted line is naive mean-field result, while the solid line is a fitting curve obtained as explained in the text.

$W = 1.2\, l^\star$ dispersion as compared to the $W = 0$ one (compare Figs. 4 and 6.) This is expected because the confining potential softens as W increases.

We also study the $\nu = 1/3$ case for Thomas-Fermi interaction. Fig. 9 and 10.) It is harder to filter out the spurious modes in this case than for (short-range) Gaussian interaction, although our scheme still works reasonbly well. The dispersions look qualitatively similar, though there is a significant change in the energy scale. This can be traced to the extra factor of 2π in the normalization of the Thomas-Fermi interaction, and has no fundamental significance.

We repeated our calculations for $\nu = 1/5$, corresponding to $s = 2, p = 1$, or $c = \sqrt{4/5}$. Since there is no substantive difference between the long- and short-range interactions between electrons, we concentrate on the short-range interaction. Results are shown in Figs. 11 and 12. There is only one edge mode, as expected.

Let us now turn to the case of fully polarized $\nu = \frac{2}{5}$, for which we present the first explicit treatment of collective edge modes, to the best of our knowledge. In this case, $s = 1$ and $p = 2$, or $c = \sqrt{4/5}$ in equations (3,3), the calculations are more involved as the bulk is filled with two CF-LLs. One needs to now consider a TDHF matrix of twice the dimension as in the case of $\frac{1}{3}$, since now there are two filled CF-LLs in which the hole can be located. There are consequently two gapless modes around the edge, propagating in the same direction. We are forced to restrict our computations to 8 CF-LLs only due to the abovementioned doubling of dimension. Figure 14 shows the imaginary part of the filtered density correlator at $Q_y = 0.4$ and 0.5. For each value of Q_y two physical peaks are evident. The dispersions for both modes are produced in Figs. 15 and 16. The mode velocity is approximately the same for both modes. It also appears, somewhat counterintuitively, that the mode with the smaller energy has greater weight in the density spectral function, indicating that it is more charged. Once again the dispersions can be fit to the heuristic form obtained earlier, as shown in Fig. .

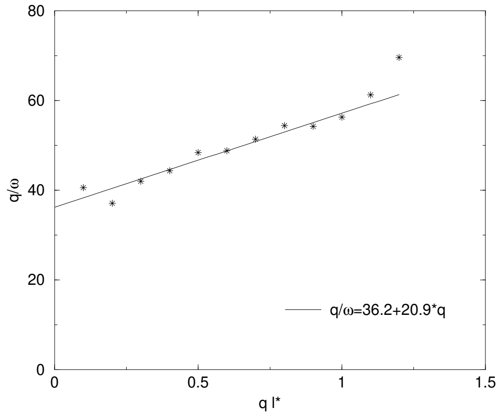

FIG. 5: Inverse of CF cyclotron velocity of $\nu = 1/3$ at width $W = 0$, Gaussian interaction, 10 CF-LLs. The solid line is linear regression for data up to $q\,l^{\star} = 1$.

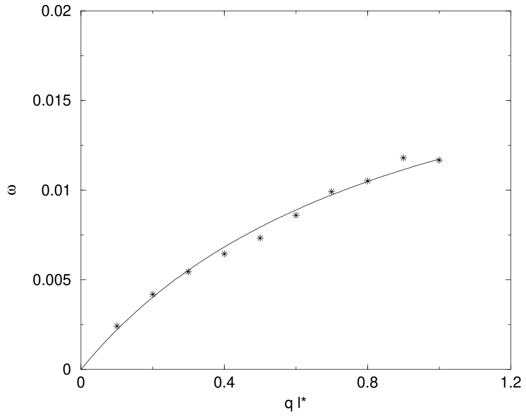

FIG. 6: Dispersion of $\nu = 1/3$ edge mode at width $W = 1.2\,l^{\star}$, Gaussian interaction, 10 CF-LLs.

V. CONCLUSIONS, CAVEATS, AND FUTURE DIRECTIONS

In this paper we have presented an approach to calculating collective edge excitations in the FQH regime which is complementary to the exact diagonalization approach. We found, as expected, a single linearly dispersing mode for the Laughlin fractions $\frac{1}{3}$ and $\frac{1}{5}$, and two linearly dispersing modes for $\frac{2}{5}$. Somewhat surprisingly, the two modes had nearly the same energy, and the one with the lower energy had the greater overlap with the charge operator. We also found that the curvature of the collective mode dispersion can be accounted for satisfactorily by a heuristic form which takes into account the fact that the effective field seen by the CFs increases as the electron density decreases, as in Eq. 30. Furthermore, in our ansatz, the magnetoexciton frequency only depends on the combination $v_0\,q\,l^{*}$. Interestingly, the free parameter a is roughly equal for $\nu = 1/3$ and both branches of $\nu = 2/5$. In fact, we can collapse the $\nu = 1/3$ and two branches of $\nu = 2/5$ data, all have $s = 1$, onto a single curve by adjusting v_0 as can be seen in Fig. 17. We did not see the roton-kike minimum seen inexact diagonalizations[14], presumably because we are not close to the reconstruction transition.

Let us turn to some caveats. While our approach does not suffer from the computational limitations of exact diagonalizations, we have computational limitations of our own. We work, in principle, in the thermodynamic limit. However, in practice, we are forced to truncate the filled states on the bulk side and the empty states on the other, to put a finite resolution on our treatment of the Landau gauge index X, and on the number of CF-LLs kept in the calculation. There are two kinds of limitations we face: In the first, HF stage, we need to find the HF ground state as accurately as possible. Each step of the iterative HF calculation takes longer when the above numbers get larger. In the second, TDHF stage, the main limitation at our current levels of resolution etc, is the time taken to construct the TDHF matrix itself, which goes as N^4, where N is a measure of the number of single-particle levels kept. The diagonalization is a small fraction of the total computation time. We had originally intended to apply the TDHF approximation to reconstructed edges as well. However, we were not successful in unambiguously identifying

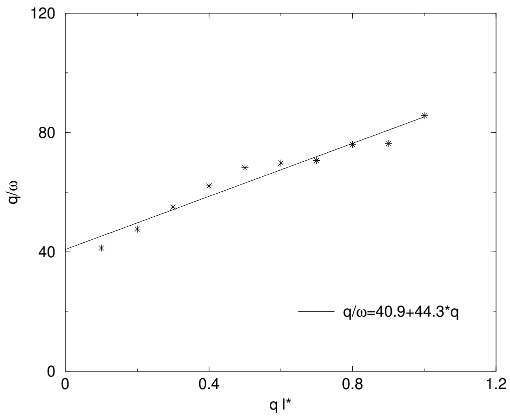

FIG. 7: Inverse of CF cyclotron velocity of $\nu = 1/3$ at width $W = 1.2\, l^{\star}$, Gaussian interaction, 10 CF-LLs. Linear regression follows.

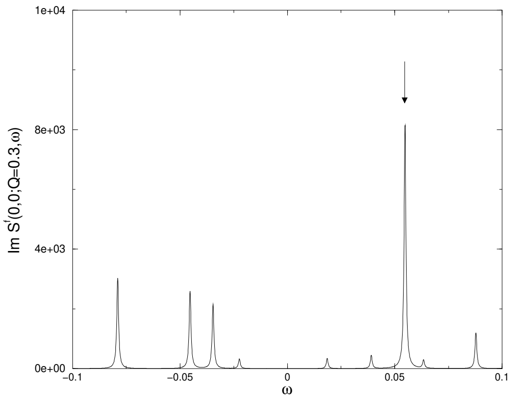

FIG. 8: Electron density-density correlator for $\nu = 1/3$ at $Q_y = 0.3$, $W = 0$, Thomas-Fermi interaction, 10 CF-LLs.

the physical modes using the spectral function, ImS^f. Presumably, if one increases the number of CF-LLs kept this task will be acheivable.

Basically, what our approach does is to bring within computational reach all the techniques which have been applied to the edge modes of the integer quantum Hall problem[26,31] to various interesting situations in the FQH regime. It does have its limitations, but despite these limitations, we believe our approach can be usefully employed for cases which cannot be solved by any competing method. Several problems illustrate our belief. If one wants to calculate

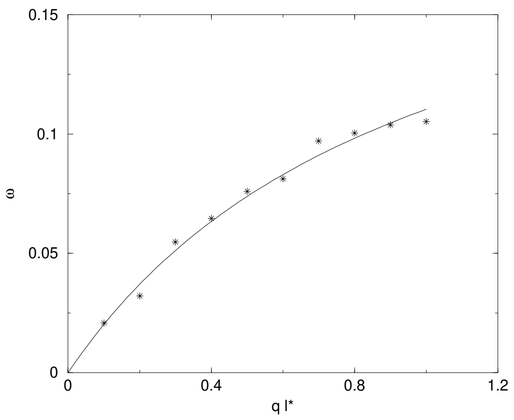

FIG. 9: Dispersion of $\nu = 1/3$ edge modes at width $W = 0$, Thomas-Fermi interaction, 10 CF-LLs.

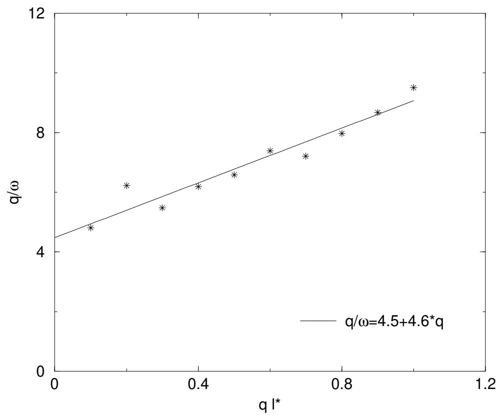

FIG. 10: Inverse of CF cyclotron velocity of $\nu = 1/3$ at width $W = 0$, Thomas-Fermi interaction, 10 CF-LLs. Linear regression follows.

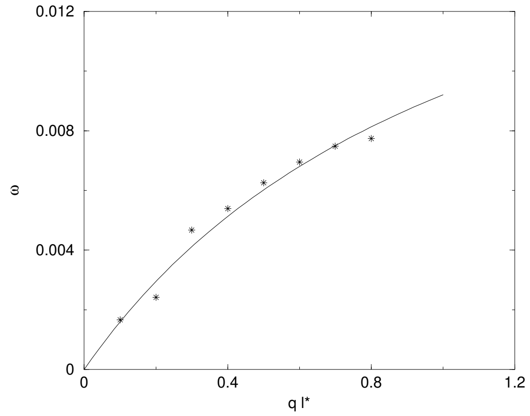

FIG. 11: Dispersion of $\nu = 1/5$ edge mode at width $W = 0$, Gaussian interaction, 10 CF-LLs. The energy is in units of $e^2/\varepsilon l^*$.

the effect of finite temperatures on the collective mode dispersions, one needs to calculate all the excited states in an exact diagonalization approach, which is computationally much more prohibitive than just finding the ground state and a few excited states. The state of the art calculation can treat 7 particles if all the states are desired to be kept[14]. One would expect the collective modes to be quite sensitive to temperature and finite size effects, since they are gapless. For example, Wan, Rezayi, and Yang[14] find that though their exact diagonalization with all states kept reproduces the qualitative features of microwave experiments[7], the energy scales are are considerably higher than that of the experiment. Secondly, in a real sample in the FQH regime, there is bound to be disorder. If the dominant disorder is due to quenched fluctuations of the remote dopant layer, then one generically expects the system to break up into incompressible strips separated by compressible regions[29]. These strips have been seen in imaging experiments[30]. It is straightforward to include the disorder potential perturbatively in our formulation, both in the HF and the TDHF approximations. The HF approximation will be somewhat more complicated because there will now be some spatial structure in the y-direction. However, using the clean single-particle and collective modes of the incompressible strip as a basis, one should be able to construct an effective theory of the collective excitations of the strip with disorder. This should provide us with a microscopic approach for examining the parameters which enter hydrodynamic approaches to this problem[8].

One can also address novel kinds of edges in our approach, such as an edge between $\frac{1}{3}$ and $\frac{2}{5}$ regions, which have CFs with the same number of vortices attached. One could further address an edge between $\frac{1}{3}$ and $\frac{2}{9}$ bulk regions, which have CFs with different numbers of vortices attached. Finally, it would be very interesting to study the dynamics of the Fermi-liquid-like state at $\nu = \frac{1}{2}$[32].

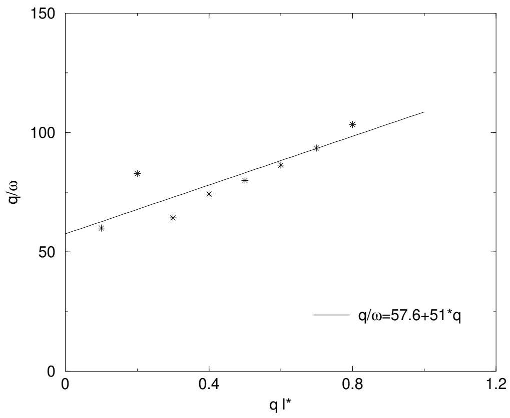

FIG. 12: Inverse of CF cyclotron velocity of $\nu = 1/5$ at width $W = 0$, Gaussian interaction, 10 CF-LLs. The fit to our heuristic form is still reasonable, though the uncertainties at in identifying the mode at small energies give larger scatter.

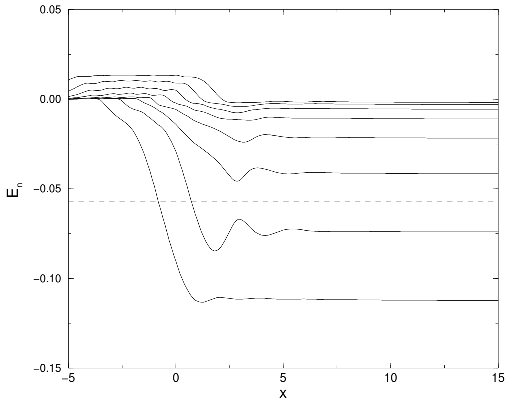

FIG. 13: Mean-field energy bands for 8 (solid) CF-LLs at $\nu = 2/5$, $W = 0$, Gaussian interaction. The energy is in units of $e^2/\varepsilon l^*$ while the x-axis is in units of l^*. The dotted line denotes the chemical potential. Two CF-LLs are occupied in the bulk.

Acknowledgments

We thank Kun Yang for helpful discussions, and the National Science Foundation for partial support under grant DMR-0311761 (HN and GM).

[1] R. B. Laughlin, Phys. Rev. Lett. **50**, 1395, (1983).
[2] J. K. Jain, Phys. Rev. Lett. **63**, 199 (1989); Phys. Rev. B **41**, 7653 (1990); Science **266**, 1199 (1994).
[3] *Perspectives in Quantum Hall Effects*, edited by S. Das Sarma and Aron Pinczuk (Wiley, New York, 1997); *Composite Fermions*, Olle Heinonen, Editor (World Scientific, 1998).
[4] B. I. Halperin, Phys. Rev. B **25**, 2185 (1982).
[5] X. G. Wen, Phys. Rev. Lett. **64**, 2206 (1990).Phys. Rev. B **41**, 12838 (1990); Int. J. Mod. Phys. B **6**, 1711 (1992).
[6] M. Grayson, D. C. Tsui, L. N. Pfeiffer, K. W. West, and A. M. Chang, Phys. Rev. Lett. **80**, 1062 (1998); A. M. Chang, M. K. Wu, C. C. Chi, L. N. Pfeiffer, and K. W. West, Phys. Rev. Lett. **86**, 143 (2001).
[7] P. D. Ye, L. W. Engel, D. C. Tsui, J. A. Simmons, J. R. Wendt, G. A. Vawter, and J. L. Reno, Phys. Rev. B **65**, 121305 (2002).
[8] C. L. Kane and M. P. A. Fisher, Phys. Rev. Lett. **68**, 1220 (1992); Phys. Rev. B **46**, 15233 (1992); Phys. Rev. B **51**, 13449 (1995).
[9] D. H. Lee and X. G. Wen, cond-mat/9809160.
[10] A. Lopez and E. Fradkin, Phys. Rev. B **59**, 15323 (1999).
[11] U. Zülicke and A. H. MacDonald, Phys. Rev. B **60**, 1837 (1999).

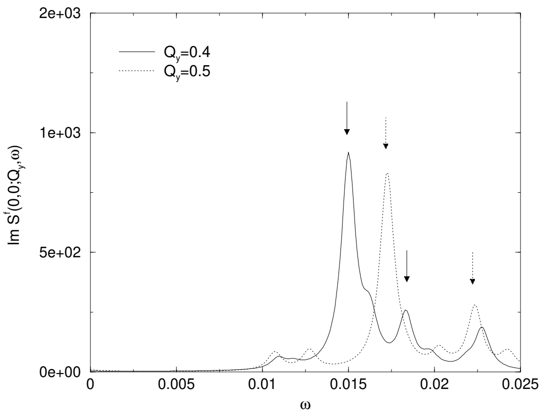

FIG. 14: Electron density-density correlator for $\nu = 2/5$ at $Q_y = 0.4$ (solid) and $0,5$ (dotted), $W = 0$, Gaussian interaction, 8 CF-LLs. The arrows indicate poles of the physical edge modes.

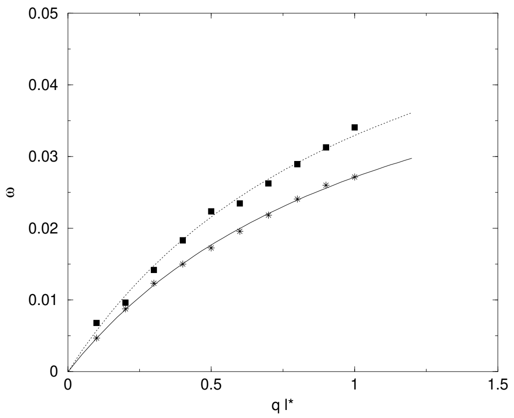

FIG. 15: Dispersions of $\nu = 2/5$ edge modes at $W = 0$, Gaussian interaction, 8 CF-LLs.

[12] L. S. Levitov, A. V. Shytov, and B. I. Halperin, Phys. Rev. B **64**, 075322 (2001).
[13] V. J. Goldman and E. V. Tsiper, Phys. Rev. Lett. **86**, 5841 (2001).
[14] X. Wan, K. Yang, and E. H. Rezayi, Phys. Rev. Lett. **88**, 056802 (2001); X. Wan, E. H. Rezayi, and K. Yang, Phys. Rev. B **68**, 125307 (2003).
[15] S. S. Mandal and J. K. Jain, Phys. Rev. Lett. **89** 096801 (2002).
[16] K. Yang, Phys. Rev. Lett. **91**, 036802 (2003).
[17] R. Shankar and G. Murthy, Phys. Rev. Lett. **79**, 4437 (1997).
[18] Y. N. Joglekar, H. K. Nguyen, and G. Murthy, Phys. Rev. B 68, 035332 (2003).
[19] G .Baym and L. P. Kadanoff, Phys. Rev. **124**, 287 (1961); L. P. Kadanoff and G. Baym, *Quantum Statistical Mechanics*, Addison-Wesley, Reading, MA, 1989.
[20] S. M. Girvin and A. H. MacDonald, Phys. Rev. Lett. **58**, 1252 (1987); S. C. Zhang, H. Hansson, and S. A. Kivelson, *ibid.* **62**, 82 (1989); N. Read, *ibid.* **62**, 86 (1989); D. H. Lee and S. C. Zhang, *ibid.* **66**, 1220 (1991).
[21] A. Lopez and E. Fradkin, Phys. Rev. Lett. **69**, 2126 (1992).
[22] J. M. Leinnas and J. Myrheim, Nuovo Cimento Soc. Ital. Fis., B **37**, 1 (1977).
[23] V. Kalmeyer and S. C. Zhang, *Phys. Rev.* **B46**, 9889, (1992).
[24] B. I. Halperin, P. A. Lee and N. Read, *Phys. Rev.* **B47**, 7312, (1993).
[25] G. Murthy and R. Shankar, Rev. Mod. Phys. **75**, 1101 (2003).
[26] C. de C. Chamon and X. G. Wen, Phys. Rev. B **49**, 8227 (1994).
[27] V. Pasquier and F. D. M. Haldane, Nucl. Phys. B **516**, 719 (1998); N. Read, Phys. Rev. B **58**, 16262 (1998).
[28] G. Murthy, Phys. Rev. B, **64**, 195310 (2001).
[29] A. L. Efros, Sol. State. Comm. **65**, 1281 (1988); Sol. State. Comm. **70**, 253 (1989); Phys. Rev. B **45**, 11354 (1992); A. L. Efros, F. G. Pikus, and V. G. Burnett, Phys. Rev. B **47**, 2233 (1993); F. G. Pikus and A. L. Efros, Phys. Rev. B **47**, 16395 (1993).
[30] See, for example, A. Yacobi *et al.*, Solid State Commun. **111**, 1 (1999).
[31] D. B. Chlovskii, B. I. Shklovskii, and L. I. Glatzman, Phys. Rev. B **46**, 4026 (1992); A. H. MacDonald, S. R. Eric Yang,

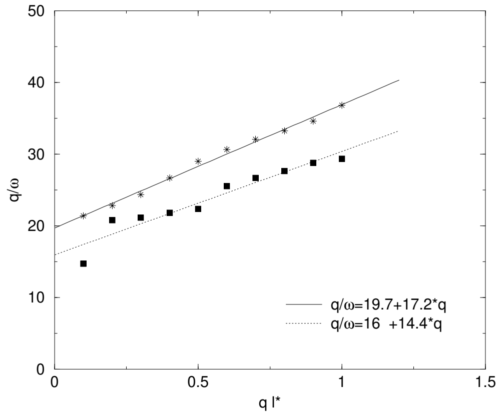

FIG. 16: Inverse of CF cyclotron velocities of $\nu = 2/5$ at width $W = 0$, Gaussian interaction, 8 CF-LLs. Linear regressions follow.

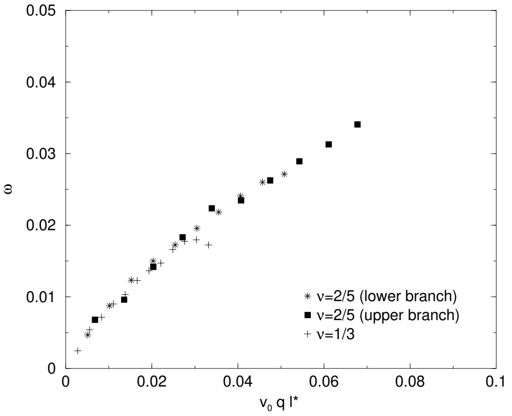

FIG. 17: Scaling of $\nu = 1/3$ and $\nu = 2/5$. v_0's are obtained by fitting data using Eq. 30.

and M. D. Johnson, Aust. J. Phys. **46**, 345 (1993); L. Brey, Phys. Rev. B **50**, 11861 (1994); D. B. Chlovskii, Phys. Rev. B **51**, 9895 (1995).

[32] S. R. Eric Yang and J. H. Han, Phys. Rev. B **57**, R12681 (1998).